

Lipolysis pathways modulate endocannabinoid biosynthesis and signaling networks in dairy cows' adipocytes

Madison N. Myers

smit2477@msu.edu

Michigan State University College of Veterinary Medicine <https://orcid.org/0000-0001-8567-8694>

Miguel Chirivi

Michigan State University College of Veterinary Medicine

Jeff C. Gandy

Michigan State University College of Veterinary Medicine

Joseph Tam

Hebrew University of Jerusalem Faculty of Medicine

Maya Zachut

Agricultural Research Organization - The Volcani Institute: Agricultural Research Organization

G. Andres Contreras


Michigan State University College of Veterinary Medicine <https://orcid.org/0000-0003-4969-2178>

Research Article

Keywords: Adipose tissue, lipolysis, endocannabinoids, endocannabinoid system, dairy cows

Posted Date: April 1st, 2024

DOI: <https://doi.org/10.21203/rs.3.rs-4138963/v1>

License:  This work is licensed under a Creative Commons Attribution 4.0 International License. [Read Full License](#)

Abstract

Background

As cows transition from pregnancy to lactation, free fatty acids (FFA) are mobilized from adipose tissues (AT) through lipolysis to counter energy deficits. In clinically healthy cows, lipolysis intensity is reduced throughout lactation; however, if FFA release exceeds tissue demands or the liver's metabolic capacity, lipid byproducts accumulate, increasing cows' risk of metabolic and infectious disease. Endocannabinoids (eCBs) and their congeners, *N*-acylethanolamines (NAEs), are lipid-based compounds that modulate metabolism and inflammation. Their synthesis and release depend upon the availability of FFA precursors and the abundance of synthesizing and degrading enzymes and transporters. Therefore, we hypothesized that eCB production and transcription of endocannabinoid system components are modulated by lipolysis pathways in adipocytes. To test this hypothesis, we stimulated canonical (isoproterenol, 1 μ M; ISO) and inflammatory (lipopolysaccharide, 1 μ g/mL; LPS) lipolysis pathways in adipocytes isolated from the AT of 5 Holstein dairy cows. Following, we assessed lipolysis intensity, adipocytes' release of eCBs, and transcription of ECS components.

Results

ISO and LPS stimulated lipolysis at comparable intensities. Exposure to ISO or LPS tended to elevate the release of eCBs and NAEs from adipocytes. ISO enhanced adipocytes' release of 2-arachidonoylglycerol (2-AG) but reduced NAE. Conversely, LPS enhanced the synthesis of *N*-arachidonylethanolamide (AEA) compared to ISO. Transcriptomic analyses revealed substantial changes in gene expression profiles amongst treatment groups. Notably, ISO enhanced the expression of 2-AG biosynthesizing genes, including *INPP5F*, *GDPD5*, and *GPAT4*. LPS augmented adipocytes' transcription of NAE-biosynthesizing *PTPN22*. LPS heightened adipocytes' transcription of 2-AG degrading *COX-2*, *MGLL*, and *CYP27B1*. Furthermore, LPS enhanced the transcription of *HSPA1A* and *SCP2* whereas ISO increased *CD36*. ISO promoted the transcription of *PPARG*, while LPS enhanced expression of *TRPV3* and *CACNA1C*.

Conclusions

Our data provide evidence for distinct modulatory roles of canonical and inflammatory lipolysis pathways over eCB release and transcriptional regulation of biosynthesis, degradation, transport, and ECS signaling in cows' adipocytes. Based on our findings, we conclude that, within adipocytes, eCB production and ECS component expression are, at least in part, mediated by lipolysis in a pathway-dependent manner. These findings contribute to a deeper understanding of the molecular mechanisms underlying metabolic regulation in dairy cows' AT, with potential implications for prevention and treatment of inflammatory and metabolic disorders.

Background

The susceptibility of dairy cows to metabolic and infectious disease is greatest during the periparturient period (PP) [1]; a physiological stage defined as the three weeks preceding and three weeks following calving [2]. To meet nutrient demands associated with lactogenesis and calving, extensive metabolic and immunologic adaptations occur – especially in cows' adipose tissues (AT) [3]. During this time, free fatty acids (FFA) are rapidly mobilized from adipocytes within AT through lipolysis, buffering energy availability according to physiologic demands [4]. This mechanism relies upon the activation of three key lipases – adipose triglyceride lipase (ATGL), hormone-sensitive lipase (HSL), and monoacylglycerol lipase (MGLL) – which sequentially break down stored lipids, releasing FFA and glycerol from AT [5]. The primary pathway, known as canonical lipolysis, is initiated upon the stimulation of growth hormone or β -adrenergic receptors (β -AR), among others, by their respective ligands [6]. Adenylyl cyclase activation triggers the phosphorylation of protein kinase A (PKA), which stimulates perilipin 1 (PLIN1) and HSL [7]. The activation of ATGL is dependent upon binding of its cofactor, α/β hydrolase domain-containing protein 5 (ABHD5), which is freed from PLIN1 upon its phosphorylation, initiating triacylglycerol hydrolysis and FFA release [8, 9].

While essential short-term, intense lipolysis that persists into lactation may result in the accumulation of toxic lipid byproducts within AT and other tissues [10, 11]. Known as lipolysis dysregulation, this process impairs local and systemic immune responses, increasing the susceptibility of near-calving cows to costly metabolic and inflammatory diseases, such as metritis, ruminal acidosis, and mastitis [11, 12]. These conditions favor the invasion of pathogenic bacteria and accumulation of bacterial fragments such as lipopolysaccharide (LPS) in the blood and peripheral tissues, which may lead to clinical endotoxemia [13]. Recent evidence published by our group demonstrates that, in bovine adipocytes, toll-like receptor-4 (TLR-4) activation by LPS triggers lipolysis through an alternative, extracellular signal-regulated kinase-1/2 (ERK1/2)-mediated cascade – a process known as inflammatory lipolysis – in addition to PKA-mediated stimulation of the canonical pathway [14, 15].

The endocannabinoid system (ECS) – a complex signaling network consisting of specialized receptors, fatty acid-derived ligands, and enzymes responsible for their synthesis, degradation, and transport – is a potent mediator of metabolic and inflammatory processes in mammals [16, 17]. Such effects result from the stimulation of diverse receptor families found within the ECS, which are widely distributed throughout the body, yet differentially expressed between cell types and tissues. For example, the metabolically active cannabinoid-1 receptor (CB1R), a G protein-coupled receptor (GPR), is highly expressed throughout nervous tissues and the surfaces of peripheral cells, including adipocytes. In the adipocytes of dairy cows, specifically, activation of CB1R enhances lipid storage and reduces FFA mobilization [18, 19]. In contrast, the cannabinoid-2 receptor (CB2R) modulates inflammatory responses and is predominantly expressed on the surface of immune cells [18, 20]. In cows exhibiting greater PP lipolysis, AT expression of *CNR1* and *CNR2* (corresponding to CB1R and CB2R, respectively) are enhanced, although the direct role lipolysis plays in the regulation of ECS-associated gene transcription is, to the authors' knowledge, yet to be revealed [21]. Additional ECS receptors include GPR (GPR18, -55, -119) [22, 23], ion channels such as

transient potential vanilloid channels-1 and -3 (TRPV1, -3) [24] and voltage-dependent calcium channels (Ca²⁺) [25], and the transcription factor peroxisome proliferator-activated receptor gamma (PPAR γ) [26, 27].

The stimulation of ECS receptors is dependent upon the availability and specificity of their ligands, endocannabinoids (eCBs) and structurally similar compounds, *N*-acylethanolamines (NAEs). Molecules in the former class, eCBs, include the two well-known arachidonic acid (AA; C20:4, *n*-6)-based compounds, 2-arachidonoylglycerol (2-AG) and *N*-arachidonylethanolamide (anandamide, AEA; C20:4 NAE). These compounds, in contrast to non-eCBs (e.g., NAEs), bind and interact with CB1R and CB2R in addition to other ECS receptors, ion channels, and transcription factors [28]. The latter, NAEs, are named according to the identity of their FFA acyl chain donor, and include AEA, linoleoylethanolamide (LEA; C18:2 NAE), oleoylethanolamide (OEA; C18:1 NAE), palmitoylethanolamide (PEA; C16:0 NAE), and stearoylethanolamide (SEA; C18:0 NAE), along with others (extensively reviewed in [29]). These molecules, along with eCBs, exert local and systemic anti-inflammatory, orexigenic, and anti-nociceptive effects through their binding and activation of ECS receptors, which may be of benefit to PP cows, especially [30].

Several factors, including cellular stress or injury, inflammation, and changes in metabolic status (e.g., fed versus fasting conditions), may stimulate the production of eCBs and NAEs [31]. Initially, biosynthesis of the compounds begins with the cleavage of FFA from an intracellular lipid source by lipases (DAGL α/β), phospholipases (NAPE-PLD, PLC), lysophospholipases (ABHD4), *N*-acyltransferases (NAT), or phospholipid phosphatases (PLPP). In non-adipocytes, the plasma membrane is considered the primary site of eCB synthesis and its resident phospholipids (PL), the primary sources of precursor FFA [32, 33]. In adipocytes, however, wherein hydrolysis of TAG by neutral lipases (ATGL, HSL) and FFA mobilization from the lipid droplet are near-constant, the effects of lipolysis on eCB biosynthesis are yet to be determined. Considering that lipolysis and inflammation are known modulators of intra- and extracellular FFA abundance and membrane PL composition, we anticipate that the biosynthesis and release of eCBs and NAEs are altered upon the stimulation of AT lipolysis pathways in the adipocytes of PP cattle [34, 35]. Such notions are supported by the previous work of Zachut et al., which revealed that greater body fat mobilization (e.g., lipolysis) post-calving is associated with elevations in AT AA, 2-AG, and AEA concentrations [21]. In the same study, PEA and OEA levels were also enhanced in AT and plasma from pre- to postpartum, corresponding with transient shifts in availability of the respective precursor FFA (palmitic, C16:0; oleic, C18:1) released from the AT of PP cows [11].

Both eCBs and NAEs are susceptible to rapid breakdown by hydrolyzing and oxidizing enzymes present in AT [17]. Hydrolysis of 2-AG is performed by ABHD6, -12, and monoglyceride lipase (MGLL), whereas fatty acid amide hydrolase (FAAH) and *N*-acylethanolamine acid amidase (NAAA) hydrolyze NAEs. Unsurprisingly, many oxidative enzymes upregulated during inflammation and intense lipolysis, including cyclooxygenases (COX-), lipoxygenases (LOX-), and cytochrome P450 monooxygenases (CYP-), degrade the FFA-based ligands and may regulate their concentrations in bovine AT [6, 11, 36]. Taken together, byproducts of eCB and NAE degradation may reciprocally modulate lipolysis intensity and inflammation in the AT of PP cows, although much remains unknown in this context [11, 17].

While greater body fat mobilization (e.g., lipolysis) and inflammation post-calving are associated with elevated eCB concentrations in cows' AT, plasma, and endometrial tissues, the direct implications of canonical and inflammatory lipolysis pathway activation on eCB production, degradation, and signaling in AT remain unknown [16, 21]. We hypothesized that stimulation of lipolysis pathways enhances the biosynthesis and release of eCBs and NAEs in bovine adipocytes by enhancing FFA availability and altering the transcriptional profile of ECS-associated gene networks (Diagram 1). Using an *in vitro* adipocyte culture model, we tested this hypothesis by determining the effects of canonical and inflammatory lipolysis pathway stimulation on eCB release and transcriptional changes in eCB- and NAE-synthesizing, degrading, transporting, and receptor gene networks.

Methods

Animals and tissue collections

All procedures were approved by the Institutional Animal Care and Use Committee at Michigan State University (AUF #11-16-188-00) and performed in accordance with local and federal guidelines.

Five healthy, multiparous, non-gestating, non-lactating Holstein cows were selected from a local abattoir. Before slaughter, animals were assigned a body condition score (BCS) by a trained veterinarian. Only cows with a BCS between 3.0 and 4.0 were considered for this study. Following euthanasia by captive bolt and jugular exsanguination, internal organs of candidate animals were evaluated. Animals with evidence of intra-abdominal, thoracic, or gastrointestinal disease were excluded. Following hide removal, 5 grams of subcutaneous AT was collected from the right paralumbar fossa (flank) region. AT samples were immediately added to 30 mL filtered Krebs-Ringer bicarbonate buffer (KRBB, pH 7.4) formulated as previously described [19]. Samples were transported at 37°C.

Adipocyte progenitor isolation and adipocyte culture

Upon arrival at the laboratory, ~ 50 mg of each AT sample was finely minced using sterile surgical scissors into 1–2 mm³ fragments. Tissue pieces were transferred into a 12-well culture plate (four fragments per well) and spaced approximately 5 mm apart. After 10 minutes of incubation at 37°C, 300 μ L of MesenPro RS Complete Medium (Thermo Fisher Scientific, Waltham, MA, USA) supplemented with 1% L-glutamine (Gibco, Waltham, MA, USA) and 0.25 μ g/mL amphotericin B (Antibiotic/Antimycotic solution; Gibco) was carefully added to each well and plates were incubated at 37°C. Medium was changed every 48 hours until preadipocytes migrated onto the plate surface from AT fragments and reached confluency. Following, cells were lifted by Trypsinization (Gibco) and passed into flasks containing preadipocyte medium consisting of 10% fetal bovine serum (FBS; Corning), Dulbecco's modified Eagle medium/F12 (Corning, Corning, NY, USA), 44.05 mM sodium bicarbonate (Corning), 100 μ M ascorbic acid (Sigma-Aldrich, St. Louis, MO, USA), 33

μ M biotin (Sigma-Aldrich), 17 μ M pantothenate (Sigma-Aldrich), 20 mM HEPES (Teknova, Hollister, CA, USA), 1% L-glutamine (Gibco), and supplemented with 100 U/mL penicillin, 100 μ g/mL streptomycin, 0.25 μ g/mL amphotericin B (Antibiotic/Antimycotic Solution; Gibco).

Following expansion (2 to 3 serial passages), preadipocytes were seeded at a density of 20,000 cells/cm² in 6-well plates [37]. Once confluency was reached, preadipocyte medium was removed and replaced with adipocyte induction medium: pre-adipocyte medium supplemented with 10 mg/mL insulin (Sigma-Aldrich), 1 μ M octanoic acid (Acros Organics, Geel, Belgium), 10 mM acetate (Sigma-Aldrich), 10 μ g/mL transferrin (Sigma-Aldrich), 5 μ M troglitazone (AdipoGen Life Sciences, San Diego, CA, USA) supplemented with 1 μ M 3-isobutyl-1-methylxanthine (IBMX; AdipoGen), and 0.5 μ M dexamethasone (Cayman Chemical, Ann Arbor, MI, USA). Following 48 hours of incubation, 60% of the induction medium volume was removed and replaced with an equivalent volume of adipocyte medium (preadipocyte medium with 10 mg/mL insulin, 1 μ M octanoic acid, 10 mM acetate, 10 μ g/mL transferrin, and 5 μ M troglitazone). Cells were incubated at 37°C and medias were refreshed every 48 hours for 7 days.

Lipolysis assays

After 7 days of induction, mature adipocytes were incubated in serum-free culture medium consisting of KRBB + 2% BSA (Sigma-Aldrich) only (basal lipolysis; BAS) or with 1 μ M isoproterenol (ISO) or 1 μ g/mL lipopolysaccharide (LPS). After 7 hours of incubation, cells and media were collected according to assay specifications detailed below, snap-frozen in liquid nitrogen, and stored at -80°C until further analysis.

Quantification of lipolysis

Lipolytic responses of adipocytes were assessed using the Glycerol-Glo kit (Promega Corp., Madison, WI, USA). Briefly, 50 μ L of treated sample medium was added to a 96-well plate, followed by 1 hour of incubation with assay reagents according to the manufacturer's guidelines. Glycerol release was normalized by protein content for each sample following extraction in RIPA buffer (Teknova) supplemented with protease and phosphatase inhibitor cocktail (Thermo Fisher Scientific), as determined by Pierce™ BCA reagent quantification [38].

Endocannabinoid quantification

Solid phase extraction began with 1:1 dilution of media samples (1 mL) in 1 HPLC-grade water (1 mL). Next, 20 μ L of methanol containing 10 ng of each internal eCB and NAE standard (arachidonoyl ethanolamide-d₈, 1-arachidonoyl-d₅-rac-glycerol, 1-arachidonoyl-d₈-rac-glycerol, and 2-arachidonoyl-glycerol-d₈, palmitoyl ethanolamide-d₅, oleoyl ethanolamide-d₄, stearoyl ethanolamide-d₃, linoleoyl ethanolamide-d₄; 0.5 μ g/ml each in methanol; Cayman Chemical) was added to each diluted sample. Following thorough mixing, samples were sonicated for 2 minutes, then carefully transferred to Oasis® PRiME HLB solid phase extraction cartridges (3 mL, 150 mg Sorbent; Waters Corporation, Milford, MA, USA) and allowed to drip through for 5 minutes. Next, cartridges were eluted twice with 1 mL of hexane-ethyl acetate (8:2; Sigma-Aldrich) and evaporated in a SpeedVac (Thermo Fisher Scientific). After, cartridges were eluted with 100 μ L of methanol, and extract suspensions were thoroughly vortexed. Then, 20 μ L water containing LC/MS-grade ammonium formate 10 mM (6.3 mg/mL water; Sigma-Aldrich) at 10 mM and 1% formic acid (10 μ L/mL water; Sigma-Aldrich) was added to each sample.

Quantification of eCBs and NAEs was achieved using the methods described by Ney et al. [39] with some modifications. Ultra performance liquid chromatographic (UPLC) separation was performed with the Waters ACQUITY® H-class UPLC system (Waters Corp.). ACQUITY UPLC™ Bridged Ethyl Hybrid C18 columns (2.1×100 mm×1.7 μ m; Waters Corp.) were used. The UPLC instrument was operated with mobile phase A consisting of 2.0 mM ammonium acetate adjusted to pH 4.5 (Solvent A), and acetonitrile (Solvent B). For chromatographic separation, a gradient was applied. First, 30% B was held for 30 seconds, gradually increased over the next 30 seconds to 50%, then 70% over 3 minutes. The final gradient was applied over 2 minutes to reach 90% B, at which conditions samples were held for 2 minutes and 30 seconds. Following, samples were returned to initial conditions and re-equilibrated for 3 minutes. A flow rate of 0.3 mL/minute was used and columns were held at 50°C.

The UPLC system was coupled to a Waters Xevo® TQ-XS triple quadrupole mass spectrometer (Waters Corp.) with multiple reaction monitoring (MRM) used for analysis. The instrument was operated in positive electrosonic spray ionization mode with a capillary voltage of 2.7 kV, and, for each MRM stage, collision energies and cone voltages were optimized. A capillary temperature of 450°C was maintained for desolvation. Pure nitrogen gas was injected at a rate of 950 L/hour for nebulization and, within the cone, 50 L/hour.

RNA extraction

Adipocytes were rinsed twice with 1 × phosphatase buffered saline (PBS; Teknova) and lifted by trypsinization. Suspensions were transferred to 0.5 mL microcentrifuge tubes and cells were pelleted at 300×g for 3 minutes. Following, supernatants were removed by pipetting. Cells were resuspended in 200 μ L of cold 1-thioglycerol/homogenization solution (Promega Corp.), flash frozen in liquid nitrogen, and samples were stored at -80°C.

Prior to extraction, samples were thawed on ice. RNA was extracted and purified using the automated Maxwell® RSC Instrument (Promega Corp.) and simplyRNA Cells Kit (Promega Corp.) according to the manufacturer's instructions. Samples were stored at -80°C until further processing. Following, RNA purity and concentration were determined using the NanoDrop 1000 Spectrophotometer (Thermo Fisher Scientific) and an RNA integrity number (RIN) was assigned to each sample using the 4200 TapeStation automated electrophoresis instrument (Agilent, Santa Clara, CA, USA) at the Michigan State University Genomics Core (East Lansing, MI, USA). All samples met quantity and purity requirements for transcriptomic sequencing; 260/230 \geq 2.0, RIN \geq 9.5 (Novogene Corporation, Beijing, China).

Bulk RNA-seq analysis

A subset of BAS-, ISO-, and LPS-treated samples from 3 animals were randomly selected for next-generation sequencing (NGS) of sample bulk RNA (RNA-seq). Samples were then shipped to Novogene Corporation (Sacramento, CA, USA) for RNA-seq reporting. Upon arrival, quality control analyses were performed for all samples. Next, poly-T oligo-attached magnetic beads were used to purify messenger RNA from 5 µg total RNA. The resulting transcripts were fragmented, and random hexamer primers were used to reverse transcribe the first strand of cDNA. For the second strand, cDNA was synthesized using dTTP (for non-directional, paired-end library construction) [40]. Following end repair, A-tailing, adapter ligation, size selection, amplification, and purification, comparative libraries were constructed. Library quality controls were certified after quantification with the Qubit® RNA Broad-Range Assay (Thermo Fisher) and real-time PCR, and for detection of size distribution, an Agilent Bioanalyzer 2100 system (Agilent Technologies, Santa Clara, CA, USA). Quantified libraries were pooled, and samples were sequenced on the HiSeq PE150 platform based on the effective library concentration, data amount, and according to the manufacturer's instructions (Illumina, San Diego, CA, USA). Sequencing depths ranged from 29 to 59 million paired-end 100 bp reads per sample (**Supplementary Table 1**) [41]. Raw reads in FASTQ format were processed through in-house perl scripts. Clean reads were obtained following the removal of adapter-containing, ploy-N, and low-quality reads. During this step, quality scores of 20 (Q20), 30 (Q30), and guanine-cytosine (GC)-content were simultaneously evaluated. Through Hisat2 (v.2.0.5), paired-end clean reads were mapped to the cow genome ARS-UCD1.2 (https://www.ebi.ac.uk/ena/data/view/GCA_002263795.2) [42]. Mapped reads were assembled using StringTie (v.1.3.3b) [43]. The featureCounts program (v1.5.0-p3) was used to count mapped read numbers that were used for gene expression analysis [44]. All data is available in NCBI Gene Expression Omnibus under accession number (GSE***upload pending***).

Statistical analyses

Assessment of metabolomics data

Statistical analyses were performed in JMP® (v.14, SAS Institute Incorporated, Cary, NC, USA). The normality of variables was calculated using the Shapiro-Wilk test ($P < 0.05$). One-way ANOVA pairwise comparisons with Tukey's HSD were calculated and used to identify differences in glycerol, eCB, and NAE concentrations among treatment groups in Experiments 1 and 2. To determine the strength and direction of associations between lipolysis intensity (glycerol release; reported in µM/ng protein) and eCB production (expressed as pmol/µg protein), Pearson correlation coefficients, denoted as "r" with associated P -values, are reported. Calculations were performed to assess total, metabolite-specific, treatment-specific, and metabolite-treatment interactions.

RNA-seq data analysis

Differential gene expression analyses were performed based on negative binomial distributions using the DESeq2R package (v1.20.0, DESeq2R development team) [45, 46]. DESeq2-normalized gene counts were \log_2 -transformed, Student's t -tests were conducted, and Benjamini and Hochberg's approach for controlling false discovery rate (FDR) was used to adjust P -values [47]. Genes were considered differentially expressed (DEG) when the \log_2 of the fold-change exceeded 0.58 (fold-change value > 1.5) and the $-\log_{10}$ of the adjusted P -value was above 1.30103 ($P \leq 0.05$). To visualize differences among comparison groups, volcano plots were created in GraphPad Prism (v.10 for Windows, GraphPad Software, Boston, MA, USA).

Of all assessed, 183 ECS-affiliated genes were selected and grouped by function (**Supplementary Table 2**) [48]. One-way ANOVA with Fisher's LSD were then performed using DESeq2-normalized counts.

Results

Canonical and inflammatory lipolysis pathways differentially alter endocannabinoid biosynthesis and release by adipocytes

Cultured adipocytes were exposed to activators of canonical (ISO) and inflammatory (LPS) lipolysis pathways for 7 hours (Fig. 1A). Following, lipolysis intensity was assessed through the quantification of glycerol release by adipocytes (Fig. 1B). The lipolytic responses of ISO- and LPS-treated adipocytes exceeded BAS levels by 1.5- and 1.6-fold, respectively, but were not different between lipolytic agents.

We then assessed the effects of targeted lipolysis pathway stimulation on the general trends in combined eCB and NAE biosynthesis and release by adipocytes (Fig. 1C). Relative to BAS, exposure to ISO ($P < 0.09$) or LPS ($P < 0.08$) tended to enhance adipocytes' overall release of the 6 eCBs and NAEs quantified.

Next, we evaluated the impacts of canonical and inflammatory lipolysis pathway activation on adipocytes' production of individual eCB and NAE (Fig. 1D). Relative to BAS, ISO enhanced the release of AA-derived 2-AG (29.4 ± 3.5 in ISO vs. 20.1 ± 2.9 in BAS; $P < 0.05$) but not AEA (0.22 ± 0.05 in ISO vs. 0.25 ± 0.09 in BAS; $P > 0.1$). AEA release was elevated in LPS-containing adipocyte media (0.56 ± 0.16) beyond BAS ($P < 0.05$) and ISO ($P < 0.01$) levels. Relative to BAS, ISO stifled adipocytes' secretion of PEA (0.0046 ± 0.0016 in ISO vs. 0.0092 ± 0.0006 in BAS; $P < 0.05$) and tended to reduce LEA concentrations (0.25 ± 0.05 in ISO vs. 0.44 ± 0.06 in BAS; $P < 0.1$). ISO-treated adipocytes released less LEA ($P < 0.05$), OEA (3.39 ± 0.38 ; $P < 0.05$), and PEA ($P < 0.01$) relative to cells treated with LPS (0.48 ± 0.27 for LEA, 2.91 ± 0.25 for OEA, and 0.48 ± 0.27 for PEA in LPS). No differences were detected in SEA concentrations among treatment groups ($P > 0.1$).

Adipocytes' transcriptomic profiles are modulated by canonical and inflammatory lipolysis pathways

To assess transcriptional differences among BAS, ISO, and LPS, NGS bulk RNA-seq analyses were performed (Fig. 2A). PCA revealed clear separations between sample clusters among treatment groups (Fig. 2B). The greatest transcriptional differences were observed in LPS vs. ISO (1901 DEG), followed by LPS vs. BAS (619 DEG), and ISO vs. BAS (444 DEG) (Figs. 2C and 2D). Relative to ISO, exposure to LPS upregulated the expression of 787 genes and downregulated that of 1114. Transcription of 170 genes was upregulated and 244, downregulated, in LPS compared to BAS. Compared to BAS, ISO enhanced mRNA expression of 127 genes and reduced that of 317.

Lipolysis pathways differentially modulate expression of eCB-synthesizing gene networks in bovine adipocytes

To establish the role of canonical and inflammatory lipolysis pathways on the transcriptional regulation of eCB biosynthesis, we evaluated adipocytes' expression of key gene networks involved (Fig. 3A; reported as DESeq2-normalized gene counts \pm SEM with significance set at $P < 0.05$ for differences and $P < 0.1$ for tendencies).

2-AG biosynthesis:

As outlined in Fig. 3B, lipolysis pathways differentially regulated the expression of 2-AG-synthesizing genes. Relative to BAS, treatment with ISO or LPS upregulated adipocytes' transcription of *DAGLB*, and the gene's expression tended to be greater in LPS than in ISO. Upon exposure to ISO, the expression of several 2-AG synthesizing genes were upregulated versus BAS and LPS, including *GDPD5*, *GPAT3*, *GPAT4*, and *INPP5F*. The presence of LPS reduced adipocytes' expression of the ATGL-encoding gene, *PNPLA2*, relative to BAS.

NAE biosynthesis:

Next, we evaluated the expression of NAE-synthesizing enzymes (Fig. 3C). Compared to BAS and ISO, *PTPN22* expression was enhanced by LPS, and its expression tended to be greater in ISO than in BAS. Exposure to ISO reduced the number of *GDPD3* transcripts relative to BAS.

Canonical and inflammatory lipolysis differentially regulate the transcription of eCB-degrading enzymes

Next, we compared the effects of BAS, ISO, and LPS on adipocytes' expression of oxidizing and hydrolyzing enzymes (Fig. 4). Compared to BAS and ISO, LPS promoted the transcription of the hydrolyzing enzyme *MGLL* and oxidizing *PTGS2* and *CYP27B1*. Expression of *ALOX12* was reduced in ISO relative to BAS and LPS, however, its transcription was comparable amongst the latter treatments.

Transporters of endocannabinoids and free fatty acids are differentially expressed upon canonical and inflammatory lipolysis

The expression of genes involved in the transport of FFA, eCBs, and NAEs were then assessed (Fig. 5). *FABP3* expression was greater in LPS than in ISO and adipocytes exposed to either treatment exhibited elevated levels over BAS. The transcription of *FABP7* was elevated in ISO and LPS over BAS but its transcription did not differ between ISO and LPS. Adipocytes treated with ISO displayed the greatest transcription of *CD36* amongst treatment groups, and counts of the gene did not differ between LPS and BAS. Exposure to LPS enhanced adipocytes' expression of *HSP1A1* and *SCP2* compared to BAS and ISO.

ECS receptors, ion channels, and transcription factors are differentially expressed upon stimulation of lipolysis

Next, we assessed transcriptional differences among gene networks associated with the receptors, ion channels, and transcription factors with which eCBs interact (Fig. 6). Exposure to ISO enhanced adipocytes' expression of *PPARG* relative to BAS and LPS. Expression of *TRPV3* was elevated in LPS relative to BAS and ISO. Transcription of the calcium ion channel-encoding gene, *CACNA1C*, was downregulated in ISO relative to BAS, and its expression tended to be higher in LPS than BAS.

Discussion

In mammals, the ECS is a potent modulator of metabolic and inflammatory processes which is widely distributed throughout organ systems, including the AT of dairy cows [17, 19, 21]. While drastic shifts in eCB and NAE concentrations and ECS component expression occur within the AT and plasma of PP dairy cows, the factors which drive these changes and their physiologic implications remain largely unknown [17, 21, 49]. Previous studies in rodents and humans have revealed that eCBs are produced within AT and modulate adipocyte FFA mobilization by way of ECS receptor signaling [50]. The present study demonstrates for the first time, however, that lipolysis pathways selectively enhance adipocytes' production of specific eCBs, which may have significant implications for metabolic and inflammatory responses in PP dairy cows. Through lipidomic and transcriptomic analyses, we identified several enriched pathways and connections between lipolysis pathways and eCB biosynthesis, degradation, transport, and ECS signaling in dairy cows' adipocytes.

Stimulation of lipolysis pathways enhances endocannabinoid production by adipocytes

Our data confirmed that, in bovine adipocytes, lipolysis upregulates the overall production of eCBs and NAEs however, the abundances and profiles of each are dependent upon which lipolysis pathway is activated (Fig. 1) [14, 21]. Previous studies have demonstrated strong associations between eCB and NAE concentrations and the abundance of FFA substrates in the diet and plasma, suggesting that precursor availability may play a role in their biosynthesis [51–53]. However, the role of lipolysis on eCB and NAE production had not been previously explored. Our data reveals a strong link exists between lipolysis and the biosynthesis and release of eCBs and NAEs by adipocytes.

Our results indicate that adipocytes' production of 2-AG is augmented following the stimulation of canonical but not inflammatory lipolysis

(Fig. 1). Given the compound's known involvement in the upregulation of feed intake, nutrient utilization, and regulation of lipolysis, enhanced levels of 2-AG may serve as a mechanism to counter negative energy balance and AT inflammation in near-calving cows, although much remains unknown in this regard [17, 54]. In contrast, our data demonstrate that the biosynthesis and release of AEA are enhanced following inflammatory—but not canonical—lipolysis. Previous studies established that immune cells biosynthesize and secrete AEA in response to LPS; however, the present study's results are the first to evidence that a similar response is observed among adipocyte populations [55, 56]. Unlike canonical lipolysis, stimulation of the inflammatory pathway was not associated with reductions in LEA biosynthesis. These observations align with findings in human macrophages by Melis et al., who not only reported a similar increase in the release of AEA upon LPS exposure, but also proposed that, in addition to availability of precursor FFA (LA and AA), the production of AEA relies upon the degree of inflammation in the extracellular environment [57]. Taken together, these results suggest that the presence of LPS upregulates AEA production. Importantly, AEA concentrations may play a role in regulating the onset and chronic inflammation in AT [58], warranting further investigation into adipocytes' capacity to synthesize and secrete the molecule, especially in cows with endotoxemia or septicemia.

As previous studies demonstrated that NAE abundances are reflective of cellular FFA profiles, we anticipated that induction of lipolytic pathways would enhance adipocytes' production of NAEs. However, the results of our study indicate that adipocytes' production and release of OEA, PEA, and SEA are reduced during canonical lipolysis. While beyond the scope of the present study, several conditions may alter the availability of FFA precursors for the biosynthesis of eCBs and NAEs in cows' adipocytes. For example, in the AT of PP cows undergoing extensive remodeling or inflammation, adipocytes contain altered glycerolipid, glycerophospholipid, glycosphingolipid, and sterol lipid profiles whose acyl chains may serve as substrates for eCB and NAE synthesis [6, 59, 60]. In addition, lipid contents vary widely between differentiating and mature adipocytes and amongst AT depots in rodent and human models [61]. Adding to the complexity of the ECS landscape in AT, certain FFA may be preferentially incorporated into adipocytes' membrane PL, thus, altering their availability [62]. While presently unknown, future studies should trace FFA released during lipolysis and evaluate their metabolism into eCBs and NAEs. The present findings underscore the complexity of networks which govern eCB and NAE production and release and emphasize the need to characterize the involvement of additional regulatory mechanisms, such as transcription of key genes.

Canonical and inflammatory lipolysis pathways differentially upregulate the transcription of endocannabinoid synthesizing networks in adipocytes

The transcriptional patterns observed in adipocytes provide novel insight on how canonical and inflammatory lipolysis pathways regulate eCB and NAE profiles in bovine AT (Fig. 3). Corresponding with upregulations in 2-AG release, our data indicates that canonical lipolysis upregulates adipocytes' expression of key genes associated with the biosynthesis of 2-AG, including *GDPD5* and *GPAT4*, which convert lysophospholipids (2-acyl lysophosphatidic acid and 2-acyl lysophosphatidylinositol) directly into 2-AG, and *INPP5F*, which cleaves phosphatidylinositol 4,5-bisphosphate to free phosphatidylinositol, an intermediate substrate, within the cell membrane [63, 64]. Despite enhancing the transcription of the AA-freeing enzyme *PLA2G4A*, LPS reduced the release of 2-AG and expression of the 2-AG biosynthesizing (and key lipase-encoding) enzyme, *PNPLA2*, suggesting bovine adipocytes may exhibit a reduced capacity to synthesize the metabolically active compound during endotoxemia.

The results of our present experiments indicate that, in bovine adipocytes, the production of AEA is upregulated in LPS (Fig. 3). At the transcriptional level, adipocytes' expression of *PTPN22*, which cleaves phospho-AEA to AEA, is upregulated upon exposure to LPS [55]. These distinct shifts in eCB release coupled with correspondent changes in transcription suggest that, during inflammatory conditions, AA may be preferentially diverted toward AEA and away from 2-AG biosynthesis. In rodent models, AEA limits TLR-4-mediated release of inflammatory cytokines by immune cells, including TNF α , nitric oxide, IL-1 β , and prostaglandins, highlighting the molecule's capacity to attenuate inflammation [65–67]. While AEA's anti-inflammatory effects are primarily attributed to its binding and activation of CB2R, its biosynthesis may, in addition, directly limit the amount of free AA available for conversion into pro-inflammatory mediators [11, 68]. Such effects may be particularly beneficial in cows challenged with endotoxemia, wherein AT inflammation may otherwise contribute to dysregulation of lipolysis and predispose cows to disease in subsequent lactations [69, 70].

Lipolysis pathways modify endocannabinoid-degrading enzyme expression and inflammatory markers in adipocytes

Under inflammatory conditions, eCBs may be rapidly oxidized by COX, LOX, CYP450, or hydrolyzed by MGLL in AT. Importantly, byproducts of eCB oxidation include the bioactive lipid-based mediators of inflammation known as oxylipids, which are associated with increased disease risk in dairy cows [71]. While the affinities of specific enzymes for eCB substrates remain unknown, COX have been shown to display high affinities for AA-based substances [68]. The present results indicate that, when adipocytes are exposed to LPS, their transcription of *PTGS2* (COX-2) and *CYP27B1* are elevated, although 2-AG levels remain comparable to basal conditions and AEA release is enhanced (Fig. 4). While the degradation of eCBs may result in the production of pro-inflammatory compounds, the direct implications of lipolysis pathway activation on eCB degradation and oxylipid biosynthesis remain undefined and should be further evaluated through silencing of degradative genes and targeted lipidomic analyses. Additionally, the results of our study indicate that adrenergic stimulation of adipocytes does not upregulate the transcription of NAE-degrading enzymes. Collectively, these findings suggest that lower NAE abundances in adipocytes' extracellular environments may be due to reductions in the compounds' biosynthesis or transport under these conditions rather than their oxidation or hydrolysis.

Canonical and inflammatory lipolysis regulate the expression of free fatty acid and endocannabinoid transporters

During lipolysis in PP cows' AT, FFA are preferentially exported out of the cell, into circulating blood, and partitioned to the mammary gland for milk synthesis [6, 72]. This process is facilitated by the activity of FFA transporters, which may also bind and transport eCBs and NAEs. Known transporters of both FFA and eCBs include fatty acid translocase (CD36), fatty acid-binding proteins (FABP3 and FABP7), heat-shock proteins (Hsp-90), solute carriers

(SLC27-), and sterol carrier protein-2 (SCP2) [73–75]. Binding of FFA precursors to carrier proteins may alter their availability for eCB or NAE biosynthesis, and the susceptibility of the compounds to oxidative or hydrolytic degradation. The present study revealed that, during canonical and inflammatory lipolysis, adipocytes' transcription of *FABP3* and *FABP7*, which are associated with the intracellular transport of lipids, are enhanced (Fig. 5). Upon adrenergic stimulation, adipocytes' transcription of *CD36* is upregulated, corresponding with heightened release of 2-AG. Coinciding with elevations in AEA abundance; however, inflammatory lipolysis upregulates the transcription of *HSP1A1* and *SCP2*, providing further mechanistic evidence for the connection between AT inflammation and adipocytes' release of AEA. At present, the specificities of certain FFA, eCB, and NAE transporters for various substrates are unknown, however, these proteins may play key roles in the modulation of AT ECS activation and should be further investigated in future studies.

Canonical and inflammatory lipolysis pathways differentially modulate the expression of endocannabinoid system receptors in bovine adipocytes

In the present study, adipocytes' expression of *PPARG*—known as the master regulator of adipogenesis—was elevated during canonical, but not inflammatory, lipolysis (Fig. 6). This finding underscores that, within the AT of otherwise healthy cows in negative energy balance, excessive FFA mobilization may be offset through the upregulation of adipogenesis and structural remodeling of AT [6]. In contrast, the AT of transition cows challenged with bacterial infections may exhibit a reduced capacity for adipogenesis, contributing to the ectopic accumulation of FFA in AT, the blood, and the liver and progression of metabolic diseases in these animals [76]. Furthermore, our data revealed that LPS upregulates the transcription of the transient receptor potential channel, *TRPV3*, in adipocytes. This receptor, whose stimulation is associated with Ca^{2+} influx and suppression of adipogenesis, may contribute to dysregulated lipolysis and inflammation – particularly in the AT of cows afflicted with endotoxemia or septicemia [77]. These observations, largely centered around the regulation of adipogenesis, emphasize ECS receptors' potential as therapeutic targets for PP cow health and frame the need to advance knowledge in this area.

Limitations and additional considerations

While the present study elucidated the roles of lipolysis pathways in adipocytes' biosynthesis and release of eCBs, this model does not mimic the AT environment in vivo. Several AT components—such as nerve fibers, immune cells, and non-adipocyte-derived hormones (e.g., insulin and norepinephrine)—may influence ECS signaling, adipocyte lipolysis, and eCB concentrations in cows' AT [17]. For example, CB1R activation on peripheral sympathetic nerves has been shown to inhibit their release of norepinephrine, which may modulate the intensity of lipolysis exhibited by adipocytes [78]. In addition, treatment of adipocytes with ISO, a pan- β -AR agonist, does not permit the isolation of effects of specific β -AR isoforms on eCB production. Therefore, to fully elucidate the involvement of β -AR in eCB synthesis and transcriptional regulation in adipocytes, future studies should consider targeted activation of β 1-, β 2-, and β 3-AR with selective agonists. On the other hand, LPS may regulate eCB concentrations and ECS signaling within AT independent of lipolysis. For instance, exposure of AT resident immune cells (such as macrophages) to LPS is known to modulate their secretion of eCBs [79]. While beyond the scope of the present study, the complex interplay between adipocytes, other cell types, and inflammation within cows' AT on the modulation of ECS signaling warrants further investigation.

Conclusions

The results of the present study indicate that lipolysis enhances eCB production and release by bovine adipocytes, which are likely reflective of elevations in FFA substrate availability. Importantly, the profile of eCBs released by adipocytes during lipolysis differs in a pathway-dependent manner, with canonical lipolysis enhancing 2-AG but reducing NAE production, and inflammatory lipolysis promoting AEA biosynthesis by adipocytes. Collectively, our results suggest that AA may be preferentially diverted toward 2-AG or AEA biosynthesis depending on the conditions within AT and surrounding environments, and such differences may be driven by modifications to adipocytes' transcription of genes associated with eCB biosynthesis, degradation, transport, and receptor interactions. Understanding the complex interplay between lipolysis, inflammation, eCB production, and ECS signaling in AT may provide insight into current approaches to cattle management and aid in the development of novel strategies to optimize the health and productivity of PP dairy cows.

Abbreviations

2-AG: 2-arachidonoylglycerol

AA: Arachidonic acid

ABHD4: α/β hydrolase domain-containing 4, N-acyl phospholipase B

ABHD5: α/β hydrolase domain-containing 5, lysophosphatidic acid acyltransferase

ABHD6: α/β hydrolase domain-containing 6, acylglycerol lipase

AEA: Anandamide

ALOX12: Arachidonate 12-lipoxygenase, 12S type

ATGL (PNPLA2): Adipose triglyceride lipase

AUF: Animal use form

β-AR: β-adrenergic receptor

BCA: Bicinchoninic acid

BCS: Body condition score

bp: Base pair

BSA: Bovine serum albumin

Ca_v1.3: Voltage-gated T-type calcium channel

CACNA1C: Voltage-gated T-type calcium channel subunit alpha 1C

CB1R (CNR1): Cannabinoid-1 receptor

CB2R (CNR2): Cannabinoid-2 receptor

CD36: Fatty acid translocase, scavenger receptor class B member 3

COX: Cyclooxygenase

COX-2 (PTGS2): Prostaglandin-endoperoxide synthase 2

CYP: Cytochrome p450 monooxygenase

CYP27B1: Cytochrome P450 monooxygenase family 27 subfamily B member 1

DAG: Diacylglycerol

DAGLα/β: Diacylglycerol lipase alpha/beta

DEG: Differentially expressed gene

dTTP: Deoxythymidine triphosphate

ECS: Endocannabinoid system

eCB: Endocannabinoid

ERK1/2: Extracellular signal-regulated protein kinases 1 and 2

FAAH: Fatty acid amide hydrolase

FABP3/7: Fatty acid-binding protein 3/7

FC: Fold-change

FDR: False discovery rate

FFA: Free fatty acid

GEO: Gene expression omnibus

GDPD3/5: Glycerophosphodiester phosphodiesterase domain-containing protein 3/5

GPAT: Glycerol-3-phosphate acyltransferase

GPR18/55/119: G protein-coupled receptor 18/55/119

HEPES: 4-(2-hydroxyethyl)-1-piperazineethanesulfonic acid

HSL: Hormone-sensitive lipase

Hsp: Heat-shock protein

HspA1A: Heat-shock protein family A member 1A

IBMX: 3-isobutyl-1-methylxanthine

IL-1 β : Interleukin-1 beta

INPP5: Inositol polyphosphate-5-phosphatase

ISO: Isoproterenol

KRBB: Krebs-Ringer bicarbonate buffer

LEA: Linolenoyl ethanolamide

LOX: Lipoxygenase

LPS: Lipopolysaccharide

LSD: Least significant difference

MAG: Monoacylglycerol

MAPK: Mitogen-activated protein kinase

MGLL: Monoacylglycerol lipase

MRM: Multiple reaction monitoring

MS: Mass spectrometry

NAAA: N-acyl ethanolamine acid amidase

NAE: N-Acylethanolamine

NAPE-PLD (NAPEPLD): N-Acylphosphatidylethanolamine-specific phospholipase D

NAT: N-acyltransferase

NGS: Next-generation sequencing

OEA: Oleoyl ethanolamide

PBS: Phosphate-buffered saline

PCA: Principal component analysis

PEA: Palmitoyl ethanolamide

PKA: Protein kinase A

PL: Phospholipid

PLC: Phosphoinositide-specific phospholipase C

PLIN: Perilipin

PLPP: Phospholipid phosphatase

PP: Periparturient

PPAR γ : Peroxisome proliferator-activated receptor gamma

PTPN22: Protein tyrosine phosphatase non-receptor type 22

RIPA: Radioimmunoprecipitation assay buffer

RNA-seq: Bulk RNA sequencing analysis

RIN: RNA integrity number

SCP2: Solute carrier protein 2

SEA: Stearoyl ethanolamide

SEM: Standard error of the mean

TAG: Triacylglycerol

THC: Tetrahydrocannabinol

TLR-4: Toll-like receptor 4

TNF α : Tumor necrosis factor alpha

TRPV1/3: Transient receptor potential cation channel subfamily V 1/3

UPLC: Ultra performance liquid chromatography

Declarations

Ethics approval and consent to participate

All procedures were conducted under protocols approved by the Institutional Animal Care and Use Committee at Michigan State University in accordance with local and federal guidelines.

Consent for publication

All authors read and approved the final manuscript prior to submission.

Availability of data and materials

Datasets generated by this study are available upon reasonable request from the corresponding author. Bulk RNA-seq data have been uploaded to the NCBI Gene Expression Omnibus (*upload pending). The datasets supporting the conclusions of this manuscript are included within the article and its additional files, which have been uploaded to the Figshare repository, https://figshare.com/projects/Lipolysis_pathways_modulate_endocannabinoid_biosynthesis_and_signaling_networks_in_dairy_cows_adipocytes/199378 [41, 48].

Competing interests

The authors have no competing interests to declare.

Funding

This project was funded by the Michigan Animal Agricultural Alliance competitive project #AA-23-0014, United States Department of Agriculture-National Institute of Food and Agriculture projects #2019-67015-29443 and #2021-67037-34657, the United States-Israel Binational Agricultural Research Development (BARD) Fund project #IS-5167-19, and the Office for the Associate Dean of Research at Michigan State University.

Authors' contributions

Conceptualization, GAC, JT, and MZ. Investigation and data curation, GAC, JG, MC, and MNM. Data analysis, MNM, MC, and GAC. Writing – drafting, MNM and GAC; review and editing, MC, JG, JT, and MZ. Data visualization and graphics, MNM. Project administration, GAC. Funding acquisition, GAC, JT, MNM, and MZ. All authors read and approved the manuscript prior to publication.

Acknowledgements

The authors extend their sincerest gratitude to David Salcedo for sharing his expertise in bioinformatics and data visualization and the staff at West Michigan Beef Company for granting us access to their facility and their assistance with sample collection.

Authors' information

Department of Large Animal Clinical Sciences, College of Veterinary Medicine, Michigan State University, East Lansing, MI, 48824, USA: Madison N. Myers, Miguel Chirivi, Jeff C. Gandy, and G. Andres Contreras

Department of Ruminant Science, Institute of Animal Sciences, Agricultural Research Organization, Volcani Center, 7505101, Rishon LeZion, Israel: Maya Zachut

Obesity and Metabolism Laboratory, The Institute for Drug Research, School of Pharmacy, Faculty of Medicine, The Hebrew University of Jerusalem, 9112001, Jerusalem, Israel: Joseph Tam

References

1. Grummer RR: **Impact of changes in organic nutrient metabolism on feeding the transition dairy cow.** *J Anim Sci* 1995, **73**(9):2820-2833.
2. LeBlanc S: **Monitoring metabolic health of dairy cattle in the transition period.** *J Reprod Dev* 2010, **56** Suppl:S29-35.
3. Contreras GA, Sordillo LM: **Lipid mobilization and inflammatory responses during the transition period of dairy cows.** *Comp Immunol Microbiol Infect Dis* 2011, **34**(3):281-289.
4. Jarc E, Petan T: **A twist of FATE: Lipid droplets and inflammatory lipid mediators.** *Biochimie* 2020, **169**:69-87.
5. Vernon RG, Pond CM: **Adaptations of maternal adipose tissue to lactation.** *J Mammary Gland Biol Neoplasia* 1997, **2**(3):231-241.
6. Contreras GA, Strieder-Barboza C, Raphael W: **Adipose tissue lipolysis and remodeling during the transition period of dairy cows.** *J Anim Sci Biotechnol* 2017, **8**:41.
7. Grabner GF, Xie H, Schweiger M, Zechner R: **Lipolysis: cellular mechanisms for lipid mobilization from fat stores.** *Nat Metab* 2021, **3**(11):1445-1465.
8. Granneman JG, Moore HP, Granneman RL, Greenberg AS, Obin MS, Zhu Z: **Analysis of lipolytic protein trafficking and interactions in adipocytes.** *J Biol Chem* 2007, **282**(8):5726-5735.
9. Granneman JG, Moore HP, Krishnamoorthy R, Rathod M: **Perilipin controls lipolysis by regulating the interactions of AB-hydrolase containing 5 (Abhd5) and adipose triglyceride lipase (Atgl).** *J Biol Chem* 2009, **284**(50):34538-34544.
10. Ospina PA, McArt JA, Overton TR, Stokol T, Nydam DV: **Using nonesterified fatty acids and β -hydroxybutyrate concentrations during the transition period for herd-level monitoring of increased risk of disease and decreased reproductive and milking performance.** *Vet Clin North Am Food Anim Pract* 2013, **29**(2):387-412.
11. Contreras GA, Strieder-Barboza C, de Souza J, Gandy J, Mavangira V, Lock AL, Sordillo LM: **Periparturient lipolysis and oxylipid biosynthesis in bovine adipose tissues.** *PLoS One* 2017, **12**(12):e0188621.
12. Contreras GA, O'Boyle NJ, Herdt TH, Sordillo LM: **Lipomobilization in periparturient dairy cows influences the composition of plasma nonesterified fatty acids and leukocyte phospholipid fatty acids.** *J Dairy Sci* 2010, **93**(6):2508-2516.
13. Eckel EF, Ametaj BN: **Bacterial Endotoxins and Their Role in Periparturient Diseases of Dairy Cows: Mucosal Vaccine Perspectives.** In: vol. 1. Dairy: MDPI; 2020: 61-90.
14. Chirivi M, Rendon CJ, Myers MN, Prom CM, Roy S, Sen A, Lock AL, Contreras GA: **Lipopolysaccharide induces lipolysis and insulin resistance in adipose tissue from dairy cows.** *J Dairy Sci* 2022, **105**(1):842-855.
15. Chirivi M, Contreras GA: **Endotoxin activates lipolysis through TLR4 signaling in bovine adipocytes.** In: *American Dairy Science Association Annual Meeting 2022: 2022; Kansas City, Missouri, USA: Journal of Dairy Science; 2022: 336-337.*
16. Bonsale R, Seyed Sharifi R, Dirandeh E, Hedayat N, Mojtahedin A, Ghorbanalinia M, Abolghasemi A: **Endocannabinoids as endometrial inflammatory markers in lactating Holstein cows.** *Reprod Domest Anim* 2018, **53**(3):769-775.
17. Myers MN, Zachut M, Tam J, Contreras GA: **A proposed modulatory role of the endocannabinoid system on adipose tissue metabolism and appetite in periparturient dairy cows.** *J Anim Sci Biotechnol* 2021, **12**(1):21.
18. Bensaid M, Gary-Bobo M, Esclangon A, Maffrand JP, Le Fur G, Oury-Donat F, Soubrie P: **The cannabinoid CB1 receptor antagonist SR141716 increases Acrp30 mRNA expression in adipose tissue of obese fa/fa rats and in cultured adipocyte cells.** *Mol Pharmacol* 2003, **63**(4):908-914.
19. Myers MN, Abou-Rjeileh U, Chirivi M, Parales-Girón J, Lock AL, Tam J, Zachut M, Contreras GA: **Cannabinoid-1 receptor activation modulates lipid mobilization and adipogenesis in the adipose tissue of dairy cows.** *J Dairy Sci* 2023, **106**(5):3650-3661.
20. Li X, Hua T, Vemuri K, Ho JH, Wu Y, Wu L, Popov P, Benchama O, Zvonok N, Locke K *et al.*: **Crystal Structure of the Human Cannabinoid Receptor CB2.** *Cell* 2019, **176**(3):459-467 e413.
21. Zachut M, Kra G, Moallem U, Livshitz L, Levin Y, Udi S, Nemirovski A, Tam J: **Characterization of the endocannabinoid system in subcutaneous adipose tissue in periparturient dairy cows and its association to metabolic profiles.** *PLoS One* 2018, **13**(11):e0205996.
22. Ramirez-Orozco RE, Garcia-Ruiz R, Morales P, Villalon CM, Villafan-Bernal JR, Marichal-Cancino BA: **Potential metabolic and behavioural roles of the putative endocannabinoid receptors GPR18, GPR55 and GPR119 in feeding.** *Curr Neuropharmacol* 2019, **17**(10):947-960.
23. Kasatkina LA, Rittchen S, Sturm EM: **Neuroprotective and Immunomodulatory Action of the Endocannabinoid System under Neuroinflammation.** *Int J Mol Sci* 2021, **22**(11).
24. Li Y, Chen X, Nie Y, Tian Y, Xiao X, Yang F: **Endocannabinoid activation of the TRPV1 ion channel is distinct from activation by capsaicin.** *J Biol Chem* 2021:101022.
25. Boczek T, Zylinska L: **Receptor-Dependent and Independent Regulation of Voltage-Gated Ca.** *Int J Mol Sci* 2021, **22**(15).
26. Sun Y, Bennett A: **Cannabinoids: a new group of agonists of PPARs.** *PPAR Res* 2007, **2007**:23513.
27. Bouaboula M, Hilairat S, Marchand J, Fajas L, Le Fur G, Casellas P: **Anandamide induced PPARgamma transcriptional activation and 3T3-L1 preadipocyte differentiation.** *Eur J Pharmacol* 2005, **517**(3):174-181.
28. Kuipers EN, Kantae V, Maarse BCE, van den Berg SM, van Eenige R, Nahon KJ, Reifel-Miller A, Coskun T, de Winther MPJ, Lutgens E *et al.*: **High Fat Diet Increases Circulating Endocannabinoids Accompanied by Increased Synthesis Enzymes in Adipose Tissue.** *Front Physiol* 2018, **9**:1913.
29. Tsuboi K, Uyama T, Okamoto Y, Ueda N: **Endocannabinoids and related N-acylethanolamines: biological activities and metabolism.** *Inflamm Regen* 2018, **38**:28.
30. Mock ED, Gagestein B, van der Stelt M: **Anandamide and other N-acylethanolamines: A class of signaling lipids with therapeutic opportunities.** *Prog Lipid Res* 2023, **89**:101194.

31. Hillard CJ: **Circulating Endocannabinoids: From Whence Do They Come and Where are They Going?** *Neuropsychopharmacology* 2018, **43**(1):155-172.
32. Hillard CJ: **Biochemistry and pharmacology of the endocannabinoids arachidonylethanolamide and 2-arachidonylglycerol.** *Prostaglandins Other Lipid Mediat* 2000, **61**(1-2):3-18.
33. Hansen HS, Diep TA: **N-acylethanolamines, anandamide and food intake.** *Biochem Pharmacol* 2009, **78**(6):553-560.
34. Yang L, Liang J, Lam SM, Yavuz A, Shui G, Ding M, Huang X: **Neuronal lipolysis participates in PUFA-mediated neural function and neurodegeneration.** *EMBO reports* 2020, **21**(11).
35. Dinkla S, van Eijk LT, Fuchs B, Schiller J, Joosten I, Brock R, Pickkers P, Bosman GJ: **Inflammation-associated changes in lipid composition and the organization of the erythrocyte membrane.** *BBA Clin* 2016, **5**:186-192.
36. Snider NT, Walker VJ, Hollenberg PF: **Oxidation of the endogenous cannabinoid arachidonoyl ethanolamide by the cytochrome P450 monooxygenases: physiological and pharmacological implications.** *Pharmacol Rev* 2010, **62**(1):136-154.
37. Strieder-Barboza C, de Souza J, Raphael W, Lock AL, Contreras GA: **Fetuin-A: A negative acute-phase protein linked to adipose tissue function in periparturient dairy cows.** *J Dairy Sci* 2018, **101**(3):2602-2616.
38. Contreras GA, Thelen K, Schmidt SE, Strieder-Barboza C, Preseault CL, Raphael W, Kiupel M, Caron J, Lock AL: **Adipose tissue remodeling in late-lactation dairy cows during feed-restriction-induced negative energy balance.** *J Dairy Sci* 2016, **99**(12):10009-10021.
39. Ney LJ, Felmingham KL, Bruno R, Matthews A, Nichols DS: **Simultaneous quantification of endocannabinoids, oleoylethanolamide and steroid hormones in human plasma and saliva.** *J Chromatogr B Analyt Technol Biomed Life Sci* 2020, **1152**:122252.
40. Parkhomchuk D, Borodina T, Amstislavskiy V, Banaru M, Hallen L, Krobitsch S, Lehrach H, Soldatov A: **Transcriptome analysis by strand-specific sequencing of complementary DNA.** *Nucleic Acids Res* 2009, **37**(18):e123.
41. Myers MN, Chirivi M, Gandy JC, Tam J, Zachut M, Contreras GA: **Supplementary Table 1. Bulk RNA-seq read counts in bovine adipocytes following canonical and inflammatory lipolysis.** In. Figshare; 2024.
42. Mortazavi A, Williams BA, McCue K, Schaeffer L, Wold B: **Mapping and quantifying mammalian transcriptomes by RNA-Seq.** *Nat Methods* 2008, **5**(7):621-628.
43. Perteu M, Perteu GM, Antonescu CM, Chang TC, Mendell JT, Salzberg SL: **StringTie enables improved reconstruction of a transcriptome from RNA-seq reads.** *Nat Biotechnol* 2015, **33**(3):290-295.
44. Liao Y, Smyth GK, Shi W: **featureCounts: an efficient general purpose program for assigning sequence reads to genomic features.** *Bioinformatics* 2014, **30**(7):923-930.
45. Love MI, Huber W, Anders S: **Moderated estimation of fold change and dispersion for RNA-seq data with DESeq2.** *Genome Biol* 2014, **15**(12):550.
46. Anders S, Huber W: **Differential expression analysis for sequence count data.** *Genome Biol* 2010, **11**(10):R106.
47. Benjamini Y, Hochberg Y: **Controlling the False Discovery Rate: A Practical and Powerful Approach to Multiple Testing.** In., vol. 57, Series B edn. Journal of the Royal Statistical Society: Wiley for the Royal Statistical Society 1995: 289-300.
48. Myers MN, Chirivi M, Gandy JC, Tam J, Zachut M, Contreras GA: **Supplementary Table 2. Endocannabinoid system-associated genes of interest assessed in bulk RNA-seq analysis following canonical and inflammatory lipolysis in dairy cows' adipocytes.** In. Figshare; 2024.
49. Dirandeh E, Ghaffari J: **Effects of feeding a source of omega-3 fatty acid during the early postpartum period on the endocannabinoid system in the bovine endometrium.** *Theriogenology* 2018, **121**:141-146.
50. Buch C, Muller T, Leemput J, Passilly-Degrace P, Ortega-Deballon P, Pais de Barros JP, Vergès B, Jourdan T, Demizieux L, Degrace P: **Endocannabinoids Produced by White Adipose Tissue Modulate Lipolysis in Lean but Not in Obese Rodent and Human.** *Front Endocrinol (Lausanne)* 2021, **12**:716431.
51. Joosten MM, Balvers MG, Verhoeckx KC, Hendriks HF, Witkamp RF: **Plasma anandamide and other N-acylethanolamines are correlated with their corresponding free fatty acid levels under both fasting and non-fasting conditions in women.** *Nutr Metab (Lond)* 2010, **7**:49.
52. Jones PJ, Lin L, Gillingham LG, Yang H, Omar JM: **Modulation of plasma N-acylethanolamine levels and physiological parameters by dietary fatty acid composition in humans.** *J Lipid Res* 2014, **55**(12):2655-2664.
53. Kra G, Daddam JR, Moallem U, Kamer H, Mualem B, Levin Y, Kočvarová R, Nemirovski A, Contreras AG, Tam J *et al*: **Alpha-linolenic acid modulates systemic and adipose tissue-specific insulin sensitivity, inflammation, and the endocannabinoid system in dairy cows.** *Sci Rep* 2023, **13**(1):5280.
54. van Ackern I, Kuhla A, Kuhla B: **A Role for Peripheral Anandamide and 2-Arachidonoylglycerol in Short-Term Food Intake and Orexigenic Hypothalamic Responses in a Species with Continuous Nutrient Delivery.** *Nutrients* 2021, **13**(10).
55. Liu J, Wang L, Harvey-White J, Osei-Hyiaman D, Razdan R, Gong Q, Chan AC, Zhou Z, Huang BX, Kim HY *et al*: **A biosynthetic pathway for anandamide.** *Proc Natl Acad Sci U S A* 2006, **103**(36):13345-13350.
56. Jin W, Yang L, Yi Z, Fang H, Chen W, Hong Z, Zhang Y, Zhang G, Li L: **Anti-Inflammatory Effects of Fucoxanthinol in LPS-Induced RAW264.7 Cells through the NAAA-PEA Pathway.** *Mar Drugs* 2020, **18**(4).
57. Melis M, Carta G, Pintus S, Pintus P, Piras CA, Murru E, Manca C, Di Marzo V, Banni S, Tomassini Barbarossa I: **Polymorphism rs1761667 in the CD36 Gene Is Associated to Changes in Fatty Acid Metabolism and Circulating Endocannabinoid Levels Distinctively in Normal Weight and Obese Subjects.** *Front Physiol* 2017, **8**:1006.

58. Bryk M, Chwastek J, Kostrzewa M, Mlost J, Pędracka A, Starowicz K: **Alterations in Anandamide Synthesis and Degradation during Osteoarthritis Progression in an Animal Model.** *Int J Mol Sci* 2020, **21**(19).
59. McFadden JW, Rico JE: **Invited review: Sphingolipid biology in the dairy cow: The emerging role of ceramide.** *J Dairy Sci* 2019, **102**(9):7619-7639.
60. Salcedo-Tacuma D, Parales-Giron J, Prom C, Chirivi M, Laguna J, Lock AL, Contreras GA: **Transcriptomic profiling of adipose tissue inflammation, remodeling, and lipid metabolism in periparturient dairy cows (*Bos taurus*).** *BMC Genomics* 2020, **21**(1):824.
61. Liaw L, Prudovsky I, Koza RA, Anunciado-Koza RV, Siviski ME, Lindner V, Friesel RE, Rosen CJ, Baker PR, Simons B *et al*: **Lipid Profiling of In Vitro Cell Models of Adipogenic Differentiation: Relationships With Mouse Adipose Tissues.** *J Cell Biochem* 2016, **117**(9):2182-2193.
62. Vanni S, Riccardi L, Palermo G, De Vivo M: **Structure and Dynamics of the Acyl Chains in the Membrane Trafficking and Enzymatic Processing of Lipids.** *Acc Chem Res* 2019, **52**(11):3087-3096.
63. Briand-Mesange F, Pons V, Allart S, Masquelier J, Chicanne G, Beton N, Payrastre B, Muccioli GG, Ausseil J, Davignon JL *et al*: **Glycerophosphodiesterase 3 (GDE3) is a lysophosphatidylinositol-specific ectophospholipase C acting as an endocannabinoid signaling switch.** *J Biol Chem* 2020, **295**(46):15767-15781.
64. Murataeva N, Straiker A, Mackie K: **Parsing the players: 2-arachidonoylglycerol synthesis and degradation in the CNS.** *Br J Pharmacol* 2014, **171**(6):1379-1391.
65. Facchinetti F, Del Giudice E, Furegato S, Passarotto M, Leon A: **Cannabinoids ablate release of TNFalpha in rat microglial cells stimulated with lipopolysaccharide.** *Glia* 2003, **41**(2):161-168.
66. Molina-Holgado F, Lledo A, Guaza C: **Anandamide suppresses nitric oxide and TNF-alpha responses to Theiler's virus or endotoxin in astrocytes.** *Neuroreport* 1997, **8**(8):1929-1933.
67. Puffenbarger RA, Boothe AC, Cabral GA: **Cannabinoids inhibit LPS-inducible cytokine mRNA expression in rat microglial cells.** *Glia* 2000, **29**(1):58-69.
68. Andres Contreras G, De Koster J, de Souza J, Laguna J, Mavangira V, Nelli RK, Gandy J, Lock AL, Sordillo LM: **Lipolysis modulates the biosynthesis of inflammatory lipid mediators derived from linoleic acid in adipose tissue of periparturient dairy cows.** *J Dairy Sci* 2020, **103**(2):1944-1955.
69. Bradford BJ, Yuan K, Farney JK, Mamedova LK, Carpenter AJ: **Invited review: Inflammation during the transition to lactation: New adventures with an old flame.** *J Dairy Sci* 2015, **98**(10):6631-6650.
70. Contreras GA, Kabara E, Brester J, Neuder L, Kiupel M: **Macrophage infiltration in the omental and subcutaneous adipose tissues of dairy cows with displaced abomasum.** *J Dairy Sci* 2015, **98**(9):6176-6187.
71. Putman AK, Gandy JC, Contreras GA, Sordillo LM: **Oxylipids are associated with higher disease risk in postpartum cows.** *J Dairy Sci* 2022, **105**(3):2531-2543.
72. Rico DE, Razzaghi A: **Animal board invited review: The contribution of adipose stores to milk fat: implications on optimal nutritional strategies to increase milk fat synthesis in dairy cows.** *Animal* 2023, **17**(4):100735.
73. Kaczocha M, Glaser ST, Deutsch DG: **Identification of intracellular carriers for the endocannabinoid anandamide.** *Proc Natl Acad Sci U S A* 2009, **106**(15):6375-6380.
74. Oddi S, Fezza F, Pasquariello N, D'Agostino A, Catanzaro G, De Simone C, Rapino C, Finazzi-Agrò A, Maccarrone M: **Molecular identification of albumin and Hsp70 as cytosolic anandamide-binding proteins.** *Chem Biol* 2009, **16**(6):624-632.
75. Gallegos AM, Atshaves BP, Storey SM, McIntosh AL, Petrescu AD, Schroeder F: **Sterol carrier protein-2 expression alters plasma membrane lipid distribution and cholesterol dynamics.** *Biochemistry* 2001, **40**(21):6493-6506.
76. Gustafson B, Smith U: **Regulation of white adipogenesis and its relation to ectopic fat accumulation and cardiovascular risk.** *Atherosclerosis* 2015, **241**(1):27-35.
77. Cheung SY, Huang Y, Kwan HY, Chung HY, Yao X: **Activation of transient receptor potential vanilloid 3 channel suppresses adipogenesis.** *Endocrinology* 2015, **156**(6):2074-2086.
78. Ishac EJ, Jiang L, Lake KD, Varga K, Abood ME, Kunos G: **Inhibition of exocytotic noradrenaline release by presynaptic cannabinoid CB1 receptors on peripheral sympathetic nerves.** *Br J Pharmacol* 1996, **118**(8):2023-2028.
79. Liu J, Batkai S, Pacher P, Harvey-White J, Wagner JA, Cravatt BF, Gao B, Kunos G: **Lipopolysaccharide induces anandamide synthesis in macrophages via CD14/MAPK/phosphoinositide 3-kinase/NF-kappaB independently of platelet-activating factor.** *J Biol Chem* 2003, **278**(45):45034-45039.

Figures

Figure 1.

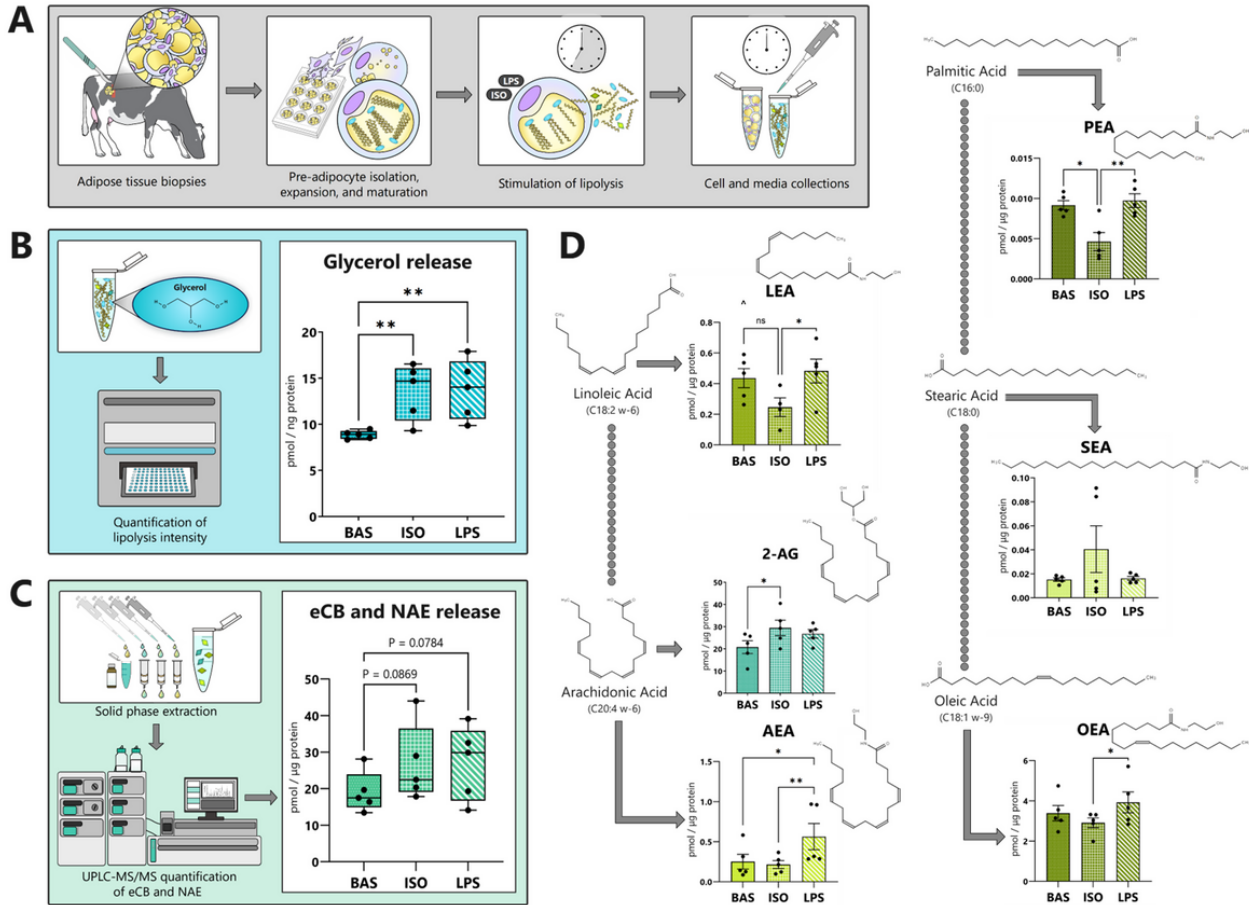


Figure 1

Lipolysis intensity and eCB abundance are modulated by canonical and inflammatory lipolysis pathways in dairy cows' adipocytes. (A) Experimental approach from adipose tissue biopsy collection to transcriptomic and metabolomic analyses. (B) Glycerol release ($\mu\text{M}/\text{ng}$ protein) by bovine adipocytes following 7 hours of canonical (ISO, $1 \mu\text{M}$), and inflammatory (LPS, $1 \mu\text{g}/\text{mL}$), and basal (BAS) lipolysis. (C) Total abundance of the endocannabinoids (eCBs), 2-arachidonylglycerol (2-AG) and *N*-arachidonylethanolamide (AEA), and the *N*-acylethanolamines (NAEs), linolenoyl ethanolamide (LEA), oleoyl ethanolamide (OEA), stearoyl ethanolamide (SEA), and palmitoyl ethanolamide (PEA), released by adipocytes into the media following lipolytic challenge. Values reported in $\text{pmol}/\mu\text{g}$ protein. (D) The influence of canonical and inflammatory lipolysis pathway activation on the release of 2-AG, AEA, LEA, OEA, PEA, and SEA by adipocytes into media. Values reported in $\text{pmol}/\mu\text{g}$ protein. Asterisks indicate differences between groups ($P < 0.1^{\wedge}$, $< 0.05^*$, $< 0.01^{**}$) as determined by ANOVA and Tukey's HSD; each dot represents an individual datapoint and error bars, SEM. $n = 5$.

Figure 2.

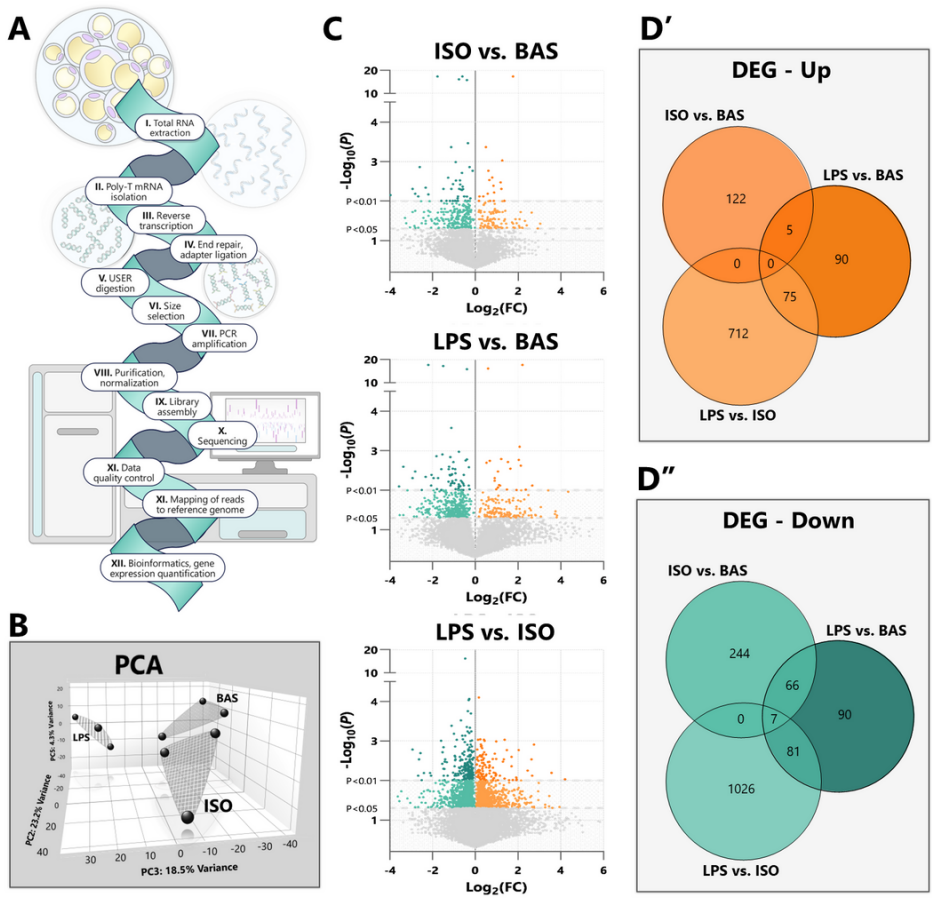


Figure 2

Canonical and inflammatory lipolysis pathways differentially alter the transcriptomic profiles of bovine adipocytes. Bovine adipocytes were exposed to isoproterenol (ISO; $1 \mu M$), lipopolysaccharide (LPS; $1 \mu g/mL$), or untreated (BAS) for 7 hours. Following, bulk RNA-seq analyses were performed ($n=3$). **(A)** Experimental workflow used. **(B)** Principal component analysis (PCA) plot depicting sample clusters exhibiting similar gene expression patterns among treated adipocyte groups. **(C)** Volcano plots of differentially expressed genes among adipocyte samples. **(D)** Venn diagrams depicting numbers of differentially expressed genes (DEG) and corresponding directional changes (D', upregulated; D'', downregulated) among comparison groups.

Figure 3.

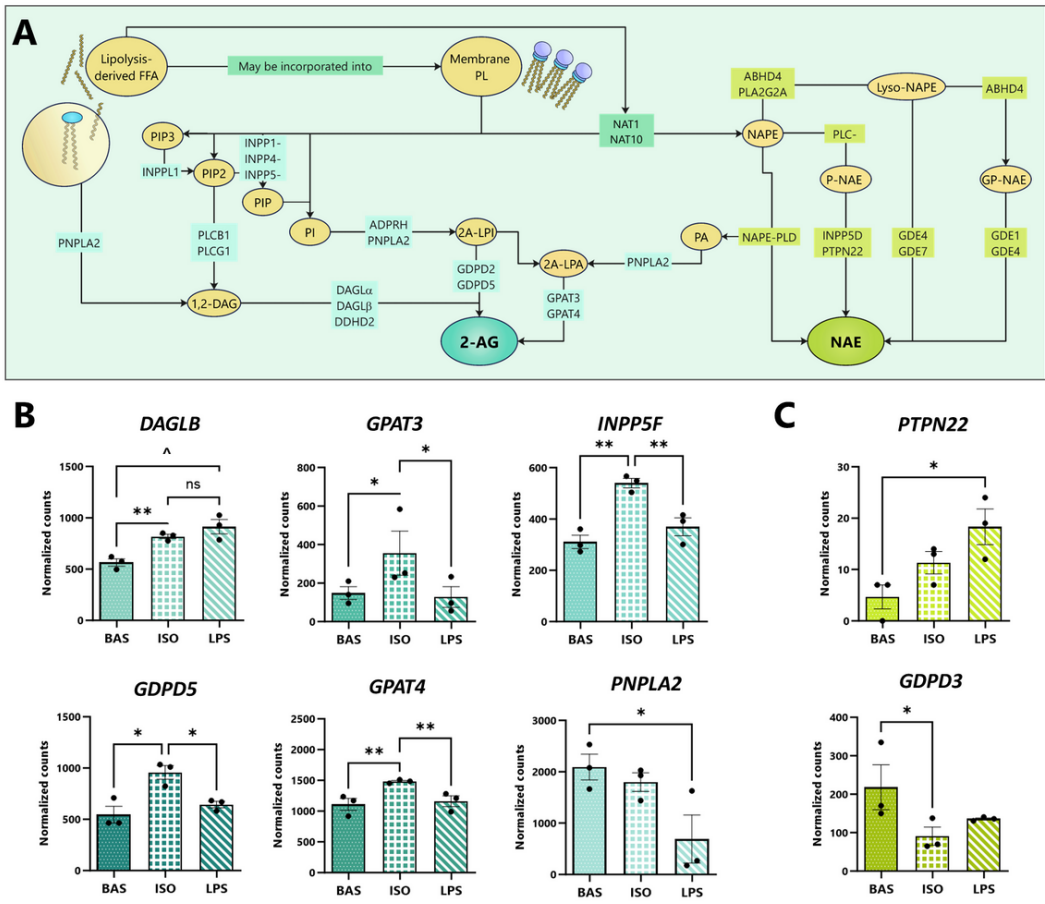


Figure 3

Lipolysis pathways alter the transcription of eCB- and NAE-synthesizing gene networks in bovine adipocytes. Bovine adipocytes were exposed to isoproterenol (ISO; 1 μ M), lipopolysaccharide (LPS; 1 μ g/mL), or untreated (BAS) for 7 hours. **(A)** Overview of eCB and NAE synthesis pathways and enzymatic catalysts which drive the reactions. **(B)** Bar graphs highlighting DESeq2-normalized gene counts associated with 2-AG biosynthesis and **(C)** NAE biosynthesis in adipocytes. Asterisks denote differences in counts between groups ($P < 0.1^{\wedge}$, $< 0.05^*$, $< 0.01^{**}$) as determined by Student's T and Fisher's LSD. Each dot represents an individual datapoint and error bars, SEM. $n=3$.

Figure 4.

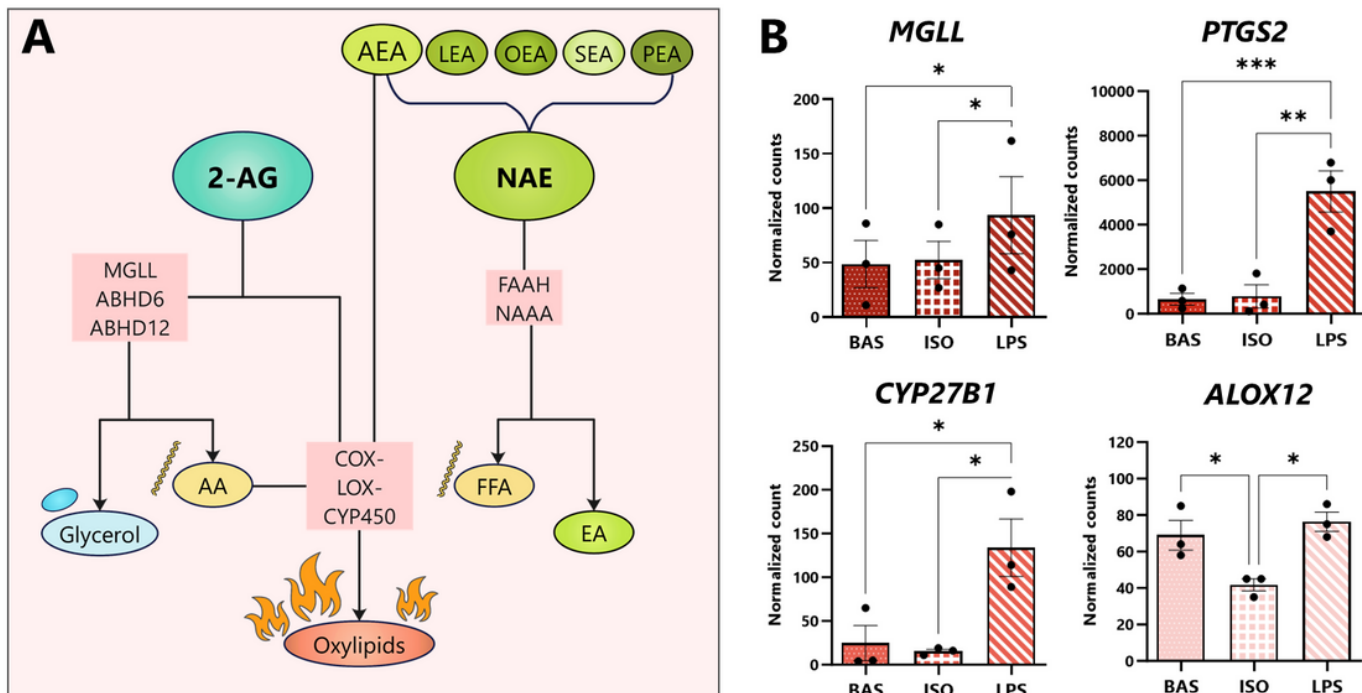


Figure 4

mRNA expression of eCB-degrading enzymes is modulated by lipolysis pathways in dairy cows' adipocytes. Bovine adipocytes were exposed to isoproterenol (ISO; 1 μM), lipopolysaccharide (LPS; 1 $\mu g/mL$), or untreated (BAS) for 7 hours. **(A)** Overview of eCB and NAE degradation pathways depicting hydrolytic and oxidative enzymes involved. **(B)** Bar graphs depicting DESeq2-normalized gene counts in cows' adipocytes following 7 hours of exposure to BAS, ISO, and LPS. Asterisks denote differences between groups ($P < 0.05^*$, $< 0.01^{**}$, $< 0.001^{***}$) as determined by Student's T and Fisher's LSD of counts; dots represent individual datapoints and error bars, SEM. $n=3$.

Figure 5.

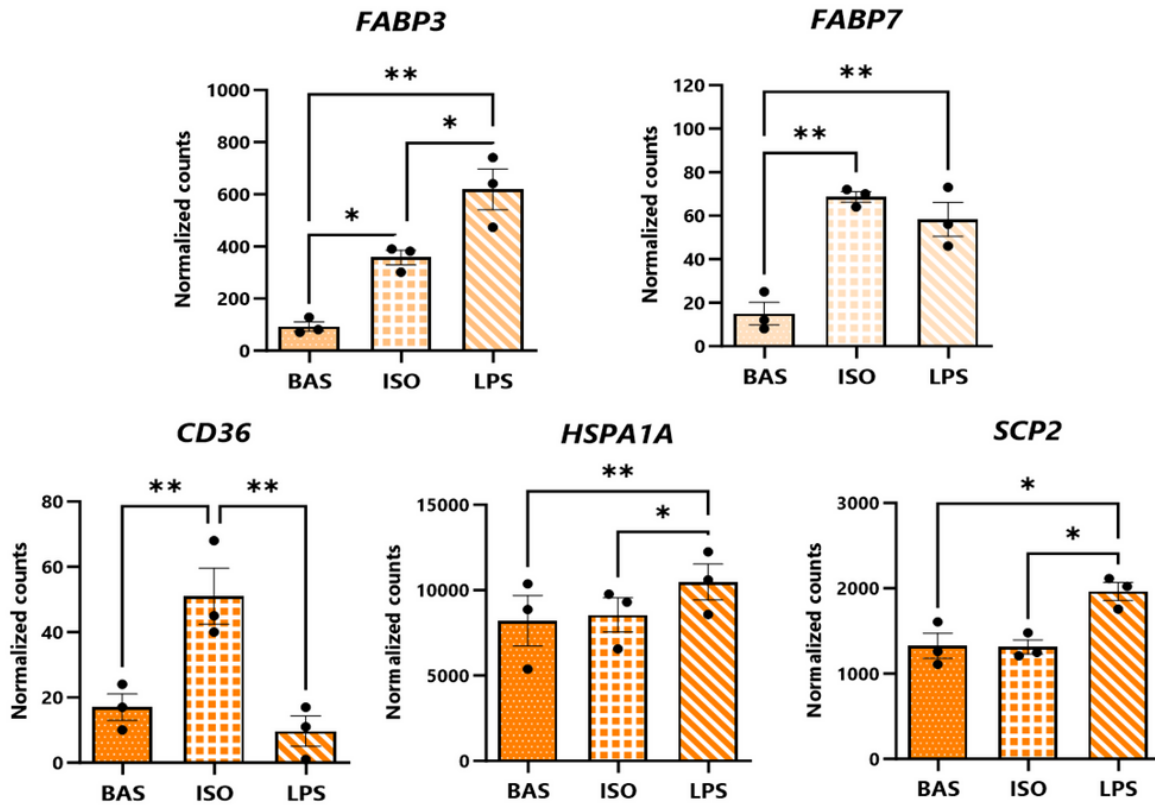


Figure 5

Transcription of FFA-, eCB-, and NAE-transporting genes is altered in dairy cows' adipocytes upon induction of lipolysis. Bar graphs of DESeq2-normalized gene counts expressed by cultured bovine adipocytes (as determined by bulk RNA-seq analysis) following 7 hours of exposure to BAS (untreated), isoproterenol (ISO; 1 μ M), and lipopolysaccharide (LPS; 1 μ g/mL). Asterisks denote differences between groups ($P < 0.05^*$, $P < 0.01^{**}$) as determined by Student's T and Fisher's LSD of counts. Dots represent individual datapoints and error bars, SEM. n=3.

Figure 6.

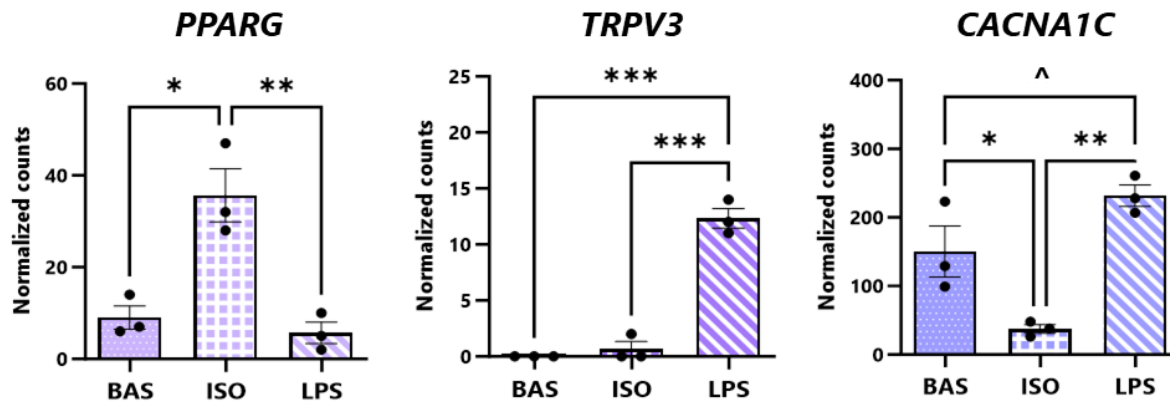


Figure 6

Expression of eCB- and NAE- interacting receptors, ion channels, and transcription factors differ upon stimulation of canonical and inflammatory lipolysis pathways. Bar graphs highlighting DESeq2-normalized gene counts expressed by bovine adipocytes following exposure to isoproterenol (ISO; 1 μ M), lipopolysaccharide (LPS; 1 μ g/mL), or untreated (BAS) for 7 hours. Asterisks denote differences between groups ($P < 0.1^{\wedge}$, $< 0.05^*$, $< 0.01^{**}$, $< 0.001^{***}$) as determined by Student's T and Fisher's LSD of counts. Dots represent individual datapoints and error bars, SEM. n=3.

Supplementary Files

This is a list of supplementary files associated with this preprint. Click to download.

- [SupplementaryTable1.pdf](#)
- [SupplementaryTable2.pdf](#)
- [Slide1.png](#)